On the prediction of the residual fatigue life of cracked structures repaired by the stop-hole method

Hao Wu [a], Abdellatif Imad [a], Noureddine Benseddiq [a], Jaime Tupiassú Pinho de Castro [b,*], Marco Antonio Meggiolaro [b]

[a] *Mechanics Laboratory of Lille, CNRS UMR 8107, Ecole Polytech'Lille, University of Lille1, Cité Scientifique, Avenue Paul Langevin, 59655 Villeneuve d'Ascq, France*
[b] *Mechanical Engineering Department, Pontifical Catholic University of Rio de Janeiro, Rua Marquês de São Vicente 225, 22453-900 Gávea, Rio de Janeiro, RJ, Brazil*

ABSTRACT

The stop-hole method is a simple and economic repair technique widely used to retard or even to stop the propagation of a fatigue crack in structural components that cannot be replaced immediately after the detection of the crack. Its principle is to drill a hole at or close to the crack tip to transform the crack into a notch, reducing in this way its stress concentration effect. The fatigue life increment that can be achieved with this technique can be modeled by assuming that it is equal to the number of cycles required to re-initiate the crack at the resulting notch root, which depends at least on the crack size and on the hole diameter. The aim of the present work is to predict the fatigue crack initiation lives by employing classical εN concepts properly modified by short crack theory to model the stop-hale effect. The comparison among the experimental and the calculation results show that the life increment caused by the stop-holes can be effectively predicted in this way.

1. Introduction

The stop-hole method is a popular emergency repair technique that has been employed for a long time to extend the fatigue life of cracked structural components that cannot be replaced as soon as the crack is discovered [1–5]. This classical resource is used by many maintenance crews all over the world, since it is relatively inexpensive, simple and fast to apply. Moreover, particularly on remote field conditions, it is frequently the last resort or the only practical option available. In its simplest form, this method consists of boring a hole in the vicinity of, or centered at the crack tip, to transform the crack into a notch. The stop-hole can in this way increase the residual fatigue life of a cracked structure in comparison to the life it would have if not repaired. However, in most practical cases the parameters and the location of the stop-hole are decided in a completely arbitrary way, totally dependent on the crew experience and skill. In consequence, sometimes the stop-hole works very well, producing significant life increments and effectively extending the cracked component replacement time. But in other cases, their results can be disappointing, or even harmful. Therefore, a simple and reliable calculation method to predict beforehand the results of this practical emergency repair technique can be quite useful in real-life situations.

However, the appropriate modeling of this problem is not that simple. Several parameters can influence the fatigue life increment caused by the stop-hole. Among them, at least the radius, the position and the surface finish of the hole; the type and the size of the crack; the geometry and the mechanical properties of the component; the history, the type and the magnitude of the load; and the residual stresses around the stop-hole border can all influence the effectiveness of the repair. The purpose of this work is to study a particular case of this complex set, the effect of the stop-hole size. As it turns out to be, even this relatively simple problem presents some quite interesting modeling challenges.

As a general rule, the increase of the stop-hole diameter contributes to decrease the value of the stress concentration factor K_t of the resulting notch, but it also increases the nominal stresses in the residual ligament of the repaired component. Indeed, the originally cracked component is transformed into a notched one after the repair, but it loses material in this process. If the stop-hole is too big, the nominal stress increase can overcome the K_t decrease, compromising its utility. On the other hand, if the stop-hole diameter is too small, the K_t reduction may not be effective. Moreover, it also may not remove the residual stresses associated with the plastic zones which always follow a fatigue crack tip. But this balance is even more delicate, since small stop-hole diameters are associated with smaller notch sensitivities q, which decrease the resulting K_t effect in the fatigue crack (re)initiation life. This effect is quantified by the so-called fatigue stress concentration factor K_f, classically defined by [6–10].

* Corresponding author. Tel.: +55 21 3527 1638; fax: +55 21 3527 1165.
E-mail address: jtcastro@puc-rio.br (J. Tupiassú Pinho de Castro).

$$K_f = 1 + q \cdot (K_t - 1) \qquad (1)$$

However, when a long crack has its tip removed by a relatively small stop-hole, it forms an elongated notch with a high K_t, which is associated with a steep stress/strain gradient around its root. Consequently, its notch sensitivity q cannot be well predicted by the classical Peterson recipe used in most fatigue textbooks, which is only appropriate to describe approximately circular or semi-circular notches [11]. Therefore, the model for predicting the residual fatigue life of repaired cracked structures must take this fact into account, as shown in the analysis presented below.

In this present work, the fatigue crack initiation lives prediction has been determined using the analytical modeling based on the classical εN and short crack theories. This investigation concerns to the case of cracked specimens which were repaired by the stop-hole method with various diameters for aluminium alloy 6082 T6. The calculation results validated by the experimental data show that the life increment caused by the stop-holes can be effectively predicted in this way.

2. Experimental program

To separate the stop-hole diameter effect from the other parameters that can influence the residual fatigue life of cracked structures repaired by this method, a set of experiments was carried out on modified SE(T) specimens, in order to measure the delays associated with the re-initiation of a fatigue crack after drilling a stop-hole centered at the fatigue crack tip. The tested material was an aluminium alloy 6082 T6, often used in industrial vehicles, railway components and shipbuilding, with chemical composition and basic mechanical properties given in Tables 1 and 2.

In these tables, S_Y is the 0.2% yielding strength, S_U is the ultimate tensile strength, E is Young's modulus, RA is area reduction and HV_{50} is the Vickers Hardness measured under a 50 kg load. The modified SE(T) specimens used for the residual life measurements were cut from the aluminium plate on the LT direction, and the fatigue tests were carried out on a 100 kN computer controlled servo-hydraulic machine, following ASTM E647 recommended procedures under constant load range ΔP at $R = P_{\min}/P_{\max} = 0.57$. This high R-ratio was chosen to guarantee that the crack was completely open at $P_{\min}$, to avoid any possible crack closure interference on the crack propagation behavior. Therefore, if a is the crack length (measured by standard potential drop techniques), $B = 8$ mm is the SE(T) thickness, $W = 80$ mm is its width, see Fig. 1, the resulting range of the stress intensity factor ΔK was calculated by [12–13]:

$$\Delta K = \frac{\Delta P}{B\sqrt{W}} \left[1.99\left(\frac{a}{W}\right)^{0.5} - 0.41\left(\frac{a}{W}\right)^{1.5} + 18.7\left(\frac{a}{W}\right)^{2.5} \right.$$
$$\left. - 38.85\left(\frac{a}{W}\right)^{3.5} + 53.85\left(\frac{a}{W}\right)^{4.5} \right] \qquad (2)$$

The 1, 2.5 or 3 mm radii stop-holes were carefully centered and drilled at the fatigue crack tips: the specimen was removed from the testing machine, fixed and positioned on a milling machine, drilled at low feedings with plenty refrigeration and then reamed to achieve a 1.5 μm diameter accuracy, and finally re-mounted on the test machine. Great care was taken to avoid overloading or introducing residual stresses around the hole by any means during this process, designed to generate notches with a same length

Table 2
The basic mechanical properties of the tested 6082 T6 Al alloy.

	S_Y (MPa)	S_U (MPa)	E (GPa)	RA (%)	HV_{50}
Al 6082 T6	280	327	68	12	95
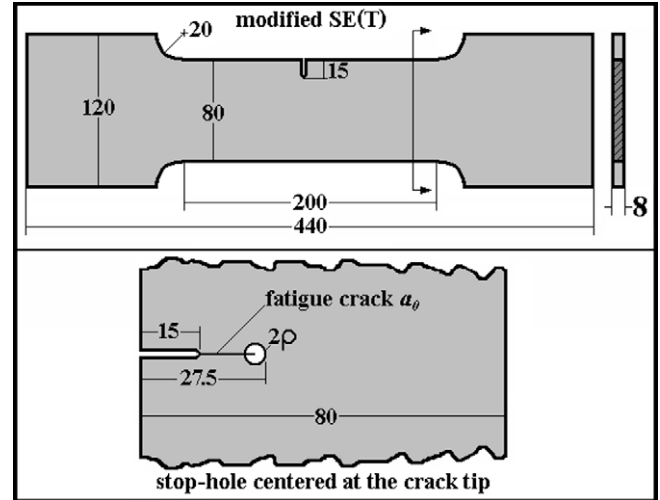
Fig. 1. The tested specimens.

$a_n = 27.5$ mm. Thus, the fatigue crack length a_0 before drilling the stop-hole depended on its radius $\rho = 1$, 2.5 or 3 mm, since the resulting notch length in all cases was fixed at $a_0 + \rho = 27.5$ mm $\Rightarrow a_n/W = 27.5/80 = 0.344$, to avoid masking the results with any possible influence of the repaired crack length a_n (or of the residual ligament size $W - a_n$). The load range ΔP was always maintained constant, before and after the drilling of the stop-holes. Table 3 summarizes the various testing conditions at the restart of the fatigue tests, after the introduction of the stop-holes.

Twenty-three specimens were tested during this work. In all of them, the fatigue crack growth was momentarily arrested after the stop-hole was drilled centered at the crack tip. This means that when re-starting the fatigue loading after repairing a specimen, a number of (delay) cycles N_d had to be spent until a new crack was able to re-initiate from the stop-hole edge, and then to start propagating again. Alternatively, it can be said that the stop-hole delayed the fatigue crack during N_d cycles, while forcing it to re-initiate from the stop-hole root. Fig. 2 shows the typical crack propagation curves measured in three specimens with different stop-hole radii, all of them tested under the same cyclic loading conditions, that is, under identical ΔP, R and a_n/W. These curves show the beneficial influence of the stop-holes (which probably would be better described as delay-holes), and of increasing the hole diameter. This benefit is quantified by the number of delay cycles N_d required to re-initiate the propagation of the repaired fatigue crack: N_d clearly increases with the hole radius ρ.

Table 4 summarizes the measured number of delay cycles N_d (which could also be called the residual fatigue life increments) caused by the stop-holes under the several testing conditions studied in this experimental program. Note that $N_d > 2 \times 10^6$ cycles means that the tests were interrupted if a fatigue crack was not

Table 1
The chemical composition of the tested 6082 T6 Al alloy.

	Si	Mg	Mn	Fe	Cr	Zn	Cu	Ti	Al
Al 6082	0.7–1.3	0.6–1.2	0.4–1.0	0.5	0.25	0.2	0.1	0.1	Balance

Table 3
Minimum, maximum and range of the loads, P_{min}, P_{max} and ΔP, and mean and range of the nominal stress, σ_m and $\Delta\sigma$, where $\sigma = P/B(W - a_n)$, associated with the applied pseudo stress intensity range $\Delta K^* = 0.838 \cdot \Delta P$ (in MPa$\sqrt{m}$, calculated by (2) using $a_n/W = 0.344$ and ΔP in kN) after introducing the stop-hole.

ΔK^* (MPa$\sqrt{m}$)	6	7.4	7.5	8	8.1	9	10.1	13.5	14
ΔP (kN)	7.163	8.835	8.954	9.551	9.671	10.75	12.06	16.12	16.71
P_{min} (kN)	16.66	20.55	20.82	22.21	22.49	24.99	28.04	37.48	38.87
P_{max} (kN)	9.496	11.71	11.87	12.66	12.82	14.24	15.98	21.37	22.16
$\Delta\sigma$ (MPa)	17.06	21.04	21.32	22.74	23.03	25.58	28.71	38.38	39.80
σ_m (MPa)	31.14	38.40	38.92	41.52	42.03	46.70	52.41	70.06	72.65
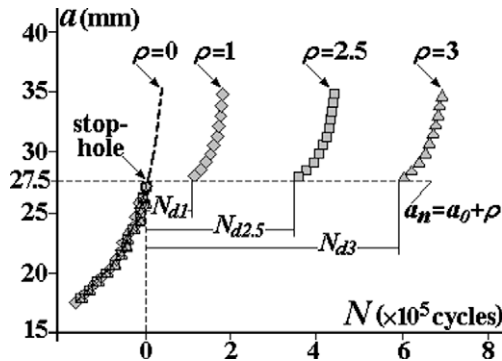
Fig. 2. Typical effect of the stop-hole on the subsequent fatigue crack propagation.

detected at the stop-hole root after this life. Note also that, as expected, the larger diameter stop-holes caused a larger number of delay cycles, as illustrated by the data measured from three specimens presented in Fig. 2 (which was obtained under $\Delta K^* = 10.1$ MPa $\sqrt{m}$ for all 3 stop-hole radii studied).

3. The basic stop-hole model

The fatigue crack re-initiation lives at the stop-hole roots can be reliably modeled by εN local strain procedures, if they are properly adjusted to describe this problem in a realistic way. This process requires (i) the cyclic properties of the 6082 T6 Al alloy,

$$H' = 443 \text{ MPa}, \quad h' = 0.064, \quad \sigma_f' = 485 \text{ MPa}, \quad b = -0.0695,$$
$$\varepsilon_f' = 0.733, \quad c = -0.827 \tag{3}$$

where σ_f', b, ε_f' and c are the Coffin–Manson parameters and H' and h' are the coefficient and the exponent of the cyclic stress–strain curve fitted by Ramberg–Osgood [14]; (ii) the nominal stress history (see Table 3); and (iii) the stress concentration factor K_t of the notches generated by repairing the cracks drilling a stop-hole at their tips. Such factors can, for example, be easily estimated by Inglis, giving for the stop-hole radii $\rho = 1, 2.5$ and 3 mm, respectively

$$K_{tl} \cong 1 + 2\sqrt{(a/\rho)} = 11.49, 7.63 \text{ or } 7.06 \tag{4}$$

The classical εN prediction models neglect the cyclic hardening or softening transient, supposing that the material fatigue behavior can be properly described by a unique Ramberg–Osgood cyclic stress/strain $\sigma\varepsilon$ curve, whose parameters H' and h' can also be used

to describe the elastic–plastic hysteresis loop $\Delta\sigma\Delta\varepsilon$ curves, which are respectively given by

$$\varepsilon = \frac{\sigma}{E} + \left[\frac{\sigma}{H'}\right]^{1/h'}, \quad \Delta\varepsilon = \frac{\Delta\sigma}{E} + 2\left[\frac{\Delta\sigma}{2H'}\right]^{1/h'} \tag{5}$$

It is advisable to use these equations to model both the nominal and the notch root cyclic stress/strain behavior, instead of assuming as usual that the nominal stresses are linear elastic. This practice avoids the logical inconsistency of using two different models for describing the same material (Hookean for the nominal and Ramberg–Osgood for the notch root stresses.), and also the significant prediction errors that can be introduced at higher nominal loads by such a regrettably widespread practice [15]. Moreover, as all the studied stop-hole radii were much bigger than the cyclic plastic zones which followed the original fatigue crack tips,

$$\rho \gg \frac{1}{\pi}\left(\frac{\Delta K}{2S_Y}\right)^2 \tag{6}$$

it is also reasonable to suppose that they did remove all the damaged material ahead of the cracks and, consequently, that the material at the resulting notch root can be treated as virgin.

Fatigue lives depend both on the range and on the maximum load components, $\Delta\sigma$ and σ_{max} (or on any equivalent combination such as σ_a and σ_m or $\Delta\sigma$ and R, e.g.). Therefore, the stop-hole problem can be modeled by first calculating the stresses and strains maxima and ranges at the notches roots according to a proper stress/strain concentration rule, which should then be used to calculate the crack re-initiation lives by an $\Delta\varepsilon \times N$ rule, considering the influence of the static or mean load component. Neglecting this effect could lead to severely non-conservative predictions, as the R-ratio used in the tests was quite high.

Thus, to consider the mean load influence on the estimated fatigue re-initiation lives after drilling a stop-hole, first it is necessary to calculate the maximum stress and strain σ_{max} and ε_{max} induced at the resulting notch root by $\sigma_{n\,max} = P_{max}/B(W - a_n) = \Delta P/B(W - a_n)(1 - R)$, the maximum nominal stress applied on the specimen after re-starting the load. This can be done by solving the Neuber/Ramberg–Osgood system along the cyclic stress/strain curve:

$$K_t^2\left[\sigma_{n\,max}^2 + \frac{E\sigma_{n\,max}^{(h'+1)/h'}}{(H')^{1/h'}}\right] = \sigma_{max}^2 + \frac{E\sigma_{max}^{(h'+1)/h'}}{(H')^{1/h'}}, \varepsilon_{max} = \frac{\sigma_{max}}{E} + \left(\frac{\sigma_{max}}{H'}\right)^{1/h'} \tag{7}$$

Table 4
Number of measured delay cycles (or residual fatigue life increments) N_d after introducing the stop-hole.

$\rho = 1$ mm		$\rho = 2.5$ mm		$\rho = 3$ mm	
ΔK^* MPa$\sqrt{m}$	$N_d \times 10^3$ cycles	ΔK^* MPa$\sqrt{m}$	$N_d \times 10^3$ cycles	ΔK^* MPa$\sqrt{m}$	$N_d \times 10^3$ cycles
6.0	>2000	7.5	>2000	8.5	>2000
7.4	980, 724, 580	8.1	1800	9.0	1150, 960
8.0	600, 560, 510	10.1	355, 270	10.1	611, 580
10.1	119, 84	13.5	65, 58, 37	14.0	60, 32

Then the stress $\Delta\sigma$ and the strain $\Delta\varepsilon$ ranges at the notch root induced by the nominal stress range caused by ΔK^* can be calculated in a similar way using the $\Delta\sigma\Delta\varepsilon$ loop equation

$$K_t^2\left[\Delta\sigma_n^2 + \frac{2E\Delta\sigma_n^{(h'+1)/h'}}{(2H')^{1/h'}}\right] = \Delta\sigma^2 + \frac{2E\Delta\sigma^{(h'+1)/h'}}{(2H')^{1/h'}},$$

$$\Delta\varepsilon = \frac{\Delta\sigma}{E} + 2\left(\frac{\Delta\sigma}{2H'}\right)^{1/h'} \tag{8}$$

Finally, the fatigue lives (to re-initiate a crack at the stop-hole root) can be estimated by one of the classical εN rules which consider $\sigma_{\max}$ or $\sigma_m = \sigma_{\max} - \Delta\sigma/2$ effects, such as

$$\frac{\Delta\varepsilon}{2} = \frac{\sigma_f' - \sigma_m}{E}(2N)^b + \varepsilon_f'(2N)^c \quad \text{(Morrow elastic)} \tag{9}$$

$$\frac{\Delta\varepsilon}{2} = \frac{\sigma_f' - \sigma_m}{E}(2N)^b$$
$$\qquad + \varepsilon_f'\left(\frac{\sigma_f' - \sigma_m}{\sigma_f'}\right)^{c/b}(2N)^c \quad \text{(Morrow elastic–plastic)} \tag{10}$$

$$\frac{\Delta\varepsilon}{2} = \frac{\sigma_f'^2}{E\sigma_{\max}}(2N)^{2b}$$
$$\qquad + \frac{\sigma_f'\varepsilon_f'}{\sigma_{\max}}(2N)^{b+c} \quad \text{(Smith–Watson–Topper)} \tag{11}$$

Since there is no consensus on which one of these three rules provides the best fatigue life estimates, it is generally advisable to conservatively analyze their predictions before taking any engineering decision, unless there is data to support a different approach. Therefore, all three rules are compared with the measured data (which in this case can thus be used to evaluate their performance). Moreover, the re-initiation lives predicted by Coffin–Manson's rule (which neglects σ_m effects) are also analyzed, to evaluate the importance of considering them on real-life applications. All the required fatigue life calculations were made using the ViDa software, a powerful and friendly general purpose software specially developed to calculate fatigue damage under general loading conditions, as described elsewhere [16]. The results of such calculations are summarized in Figs. 3–5.

The first conclusion obtainable from these plots is that the lives predicted by Morrow El, Morrow EP and SWT are similar in this case (but it must be emphasized that such a similarity regrettably cannot be assumed beforehand, since in many other cases these rules can and do predict very different fatigue lives!), whereas the Coffin–Manson predictions are highly non-conservative, thus absolutely useless. Therefore, it is indeed necessary to consider
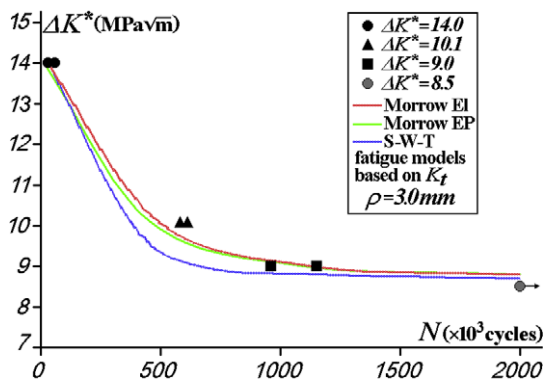
Fig. 3. Predicted and measured fatigue crack re-initiation lives at the roots of the stop-holes of radius $\rho = 3.0$ mm, using the stress concentration factor K_t of the repaired crack.
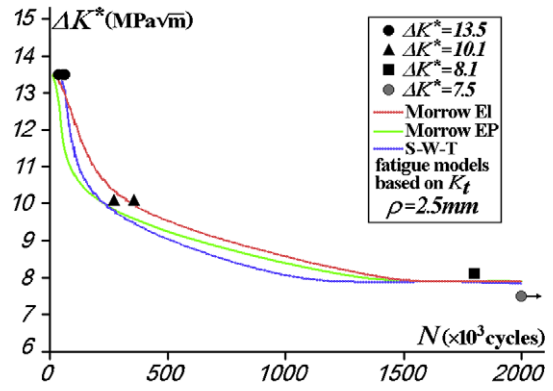
Fig. 4. Predicted and measured fatigue crack re-initiation lives at the roots of the stop-holes of radius $\rho = 2.5$ mm, using the stress concentration factor K_t of the repaired crack.
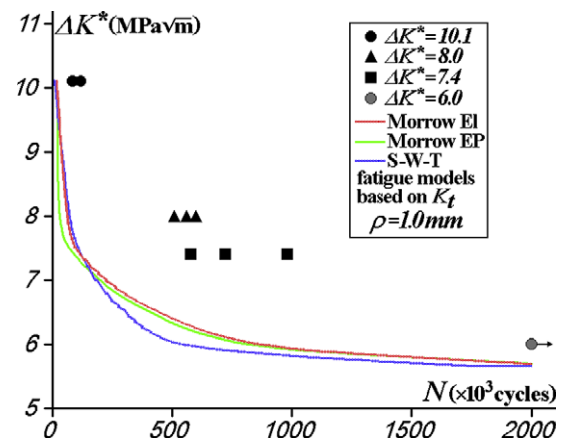
Fig. 5. Predicted and measured fatigue crack re-initiation lives at the roots of the stop-holes of radius $\rho = 1.0$ mm, using the stress concentration factor K_t of the repaired crack.

the $\sigma_{\max}$ or σ_m effects to predict the fatigue life improvement obtainable from a stop-hole, particularly when the subsequent loading has a high R-ratio.

Another important conclusion is that for the two bigger stop-holes (with radii $\rho = 3.0$ and $\rho = 2.5$ mm) the predictions reproduce quite well the measured fatigue crack re-initiation lives. In fact, so well that it is worth to point out that the curves in those plots really result from calculated life predictions, not from data fitting. But the predictions obtained by the same calculation procedures for the smaller stop-hole with $\rho = 1.0$ mm are much more conservative. This behavior is a little bit surprising, but since for design purposes this performance is not really that bad, based on the limited but representative data measured, the relatively simple procedure used above could probably be recommended as a useful design tool.

However, from a more fundamental point of view, this behavior is at least odd, and must be explained. One way of dealing with this problem is to blame it on intrinsic statistical variations, since everybody knows that fatigue initiation lives are quite disperse. But a much more sensible mechanical approach can be used to reproduce all the measured data, because there are few mechanical reasons which can explain the better than expected fatigue lives obtained from the specimens repaired by the $\rho = 1$ mm stop-holes. Significant compressive residual stresses, $\sigma_{res} \ll 0$, could be one of them. However, all the holes were drilled and reamed following identical procedures, and the bigger stop-hole lives were well predicted supposing $\sigma_{res} = 0$. Therefore, it is difficult to justify why

high compressive residual stresses would be present only at the smaller stop-holes roots. The same can be said about the surface finish of the stop-holes. But the smaller stop-holes generate a notch with a bigger K_t and, which is more important, with a much steeper stress gradient near their roots. This effect can significantly affect the growth of short cracks and, consequently, the so-called fatigue notch sensitivity [11], mechanically explaining the measured behavior, as follows.

4. Analytical prediction of the notch sensitivity

It is well known that the fatigue crack growth rate da/dN is controlled by two parameters, the stress intensity range ΔK and maximum $K_{\max}$ or, equivalently, by ΔK and $R = K_{\min}/K_{\max}$; and that the cracks grow under a given $\Delta\sigma$ and R set when $\Delta K = \Delta\sigma\sqrt{(\pi a)}\cdot f(a/w) > \Delta K_{th}(R)$, where $f(a/w)$ is the function that describes the cracked piece geometry contribution to ΔK and $\Delta K_{th}(R)$ is the (long) crack propagation threshold at that R-ratio. Therefore, as the stress intensity factor K generally increases when the crack size a augments, the short cracks (which have $a \cong 0$) must thus propagate in a way intrinsically different from the long cracks, as otherwise $\Delta K(a \to 0, R) > \Delta K_{th}(R) \Rightarrow \Delta\sigma \to \infty$, which is a non-sense, as a stress range $\Delta\sigma > 2S_L(R)$ can generate and propagate a fatigue crack, where $S_L(R)$ is the fatigue limit of the material at R. To conciliate the fatigue limit (e.g.) at $R = 0$, $\Delta S_0 = 2S_L(0)$, with the propagation threshold under pulsating loads $\Delta K_0 = \Delta K_{th}(0)$, a small "short crack characteristic size" a_0 can be summed to the actual crack size a to obtain [17].

$$\Delta K_I = \Delta\sigma\sqrt{\pi(a + a_0)} \qquad (12)$$

where $a_0 = (1/\pi)\cdot(\Delta K_0/\Delta S_0)^2$. In this way, the long fatigue cracks, with $a \gg a_0$, do not grow if $\Delta K_I = \Delta\sigma\sqrt{(\pi a)} < \Delta K_0$, while the microcracks (which size $a \to 0$) do not propagate by fatigue if $\Delta\sigma < \Delta S_0$, since in this case $\Delta K_I = \Delta\sigma\sqrt{(\pi a_0)} < \Delta S_0\sqrt{(\pi a_0)} = \Delta K_0$. This model thus reproduces the proper physical behavior in these limit cases. To consider the geometry contribution to ΔK, expressed in $f(a/w)$, the a_0 definition could be adapted by [18]

$$a_0 = \frac{1}{\pi}\left(\frac{\Delta K_0}{f(a/w)\cdot\Delta S_0}\right)^2 \qquad (13)$$

Both (12) and (13) predict that the biggest stress range which does not propagate a microcrack is the fatigue limit: if $a \ll a_0$, $\Delta K_I = \Delta K_0 \Rightarrow \Delta\sigma \to \Delta S_0$. However, when the crack departs from a notch, as usual, its driving force is the stress range at the notch root $\Delta\sigma$, not the nominal stress range $\Delta\sigma_n$, which is generally used on the ΔK expressions. As in these cases the factor $f(a/w)$ includes the stress concentration effect of the notch, it is better to define $f(a/w)$ separating it in two parts: $f(a/w) = \eta\phi(a)$, where $\phi(a)$ quantifies the stress gradient effect near the notch, with $\phi(a \to 0) \to K_t$, while the constant η quantifies the free surface effect, to obtain

$$\Delta K_I = \eta\cdot\varphi(a)\cdot\Delta\sigma_n\sqrt{\pi(a + a_0)}, \quad \text{where } a_0 = \frac{1}{\pi}\left(\frac{\Delta K_0}{\eta\cdot\Delta S_0}\right)^2 \qquad (14)$$

Using the traditional definition $\Delta K = f(a/w)\cdot\Delta\sigma\sqrt{(\pi a)}$, an alternate way to model the short crack effect is to suppose that the fatigue crack propagation threshold depends on the crack size, $\Delta K_{th}(a, R = 0) = \Delta K_{th}(a)$, through a function given by

$$\frac{\Delta K_{th}(a)}{\Delta K_0} = \frac{\Delta\sigma\sqrt{\pi a}\cdot f(a/w)}{\Delta\sigma\sqrt{\pi(a + a_0)}\cdot f(a/w)} = \sqrt{\frac{a}{a + a_0}} \Rightarrow \Delta K_{th}(a)$$
$$= \frac{\Delta K_0}{\sqrt{1 + (a_0/a)}} \qquad (15)$$

However, an additional adjustable parameter γ in the $\Delta K_{th}(a)$ expression allows a better fitting of the experimental data [19]:

$$\Delta K_{th}(a) = \Delta K_0[1 + (a_0/a)^{\gamma/2}]^{-1/\gamma} \qquad (16)$$

If S_L' and $S_L = S_L'/K_f$ are the fatigue limits measured, respectively, in standard (polished and non-notched) and in similar but notched SN specimens, the stress concentration factor of the notch $K_t \geqslant K_f$. The difference between K_f and K_t is quantified by the so-called notch sensitivity factor q, where $0 \leqslant q = (K_f - 1)/(K_t - 1) \leqslant 1$, meaning that $K_f = 1 + q(K_t - 1)$.

In mechanical design [7–10], the notch sensitivity q is still quantified by empirical curves fitted by Peterson to 7 data points in the middle of the last century [6]. But it is reasonable to expect that q can be modeled using the short crack behavior, since it can be associated to tiny cracks which can initiate at the notch root but do not propagate when $2S_L'/K_t < \Delta\sigma < 2S_L'/K_f$ [20]. For example, according to Tada [21], the stress intensity factor of a crack that departs from a circular hole of radius ρ in a Kirsh (infinite) plate loaded in mode I is given by:

$$\Delta K_I = \eta\cdot\varphi(a/\rho)\cdot\Delta\sigma\sqrt{\pi a} = 1.1215\cdot\varphi(a/\rho)\cdot\Delta\sigma\sqrt{\pi a} \qquad (17)$$

where $\phi(a/\rho) \equiv \phi(x)$, which is related to the stress gradient near the hole border, is given by:

$$\varphi(x) = \left(1 + \frac{0.2}{(1+x)} + \frac{0.3}{(1+x)^6}\right)$$
$$\cdot\left(2 - 2.354\frac{x}{1+x} + 1.206\left(\frac{x}{1+x}\right)^2 - 0.221\left(\frac{x}{1+x}\right)^3\right) \qquad (18)$$

Note that $\lim\limits_{a\to 0}\Delta K_I = 1.1215\cdot 3\cdot\Delta\sigma\sqrt{\pi a}$ and $\lim\limits_{a\to\infty}\Delta K_I = \Delta\sigma\sqrt{\pi a/2}$, exactly as expected. Thus, if $a_0 = (\Delta K_0/\eta\Delta S_0\sqrt{\pi})^2$, any crack departing from a Kirsh hole will propagate when

$$\Delta K_I = \eta\cdot\varphi(a/\rho)\cdot\Delta\sigma\sqrt{\pi a} > \Delta K_{th} = \Delta K_0\cdot[1 + (a_0/a)^{\gamma/2}]^{-1/\gamma} \qquad (19)$$

The propagation criterion for these fatigue cracks can then be rewritten as [11]

$$\varphi\left(\frac{a}{\rho}\right) > \frac{\left(\frac{\Delta K_0}{\Delta S_0\sqrt{\rho}}\right)\cdot\left(\frac{\Delta S_0}{\Delta\sigma}\right)}{\left[\left(\eta\sqrt{\frac{\pi a}{\rho}}\right)^\gamma + \left(\frac{\Delta K_0}{\Delta S_0\sqrt{\rho}}\right)^\gamma\right]^{1/\gamma}} \equiv g\left(\frac{a}{\rho}, \frac{\Delta S_0}{\Delta\sigma}, \frac{\Delta K_0}{\Delta S_0\sqrt{\rho}}, \gamma\right) \qquad (20)$$

Therefore, $K_f = \Delta S_0/\Delta\sigma$ can be calculated from the material fatigue limit ΔS_0 and crack propagation threshold ΔK_0, and from the geometry of the cracked piece by solving the system

$$\begin{cases} \varphi(a/\rho) = g(a/\rho, \Delta S_0/\Delta\sigma, \Delta K_0/\Delta S_0\sqrt{\rho}, \gamma) \\ \frac{\partial}{\partial a}\varphi(a/\rho) = \frac{\partial}{\partial a}g(a/\rho, \Delta S_0/\Delta\sigma, \Delta K_0/\Delta S_0\sqrt{\rho}, \gamma) \end{cases} \qquad (21)$$

to obtain the maximum stress range $\Delta\sigma$ that can initiate and cohabit with a non-propagating crack of size a. This system can then be solved for several combinations of materials and hole radii, specified by $\Delta K_0/\Delta S_0\sqrt{\rho}$ and γ, to obtain the Kirsh plate notch sensitivity as a function of the hole radius ρ and material fatigue properties. Fig. 6 compares the q values calculated in this way with the traditional Peterson curves normally used in mechanical design [6–10].

This analytical approach includes the γ exponent which allows a better fitting of the short crack propagation data, and it can be easily generalized to deal with other notch geometries. This generalization is important here, since the stop-hole repaired cracks are similar to an elongated semi-elliptical notch, not to a Kirsh hole. The stress intensity factor of a crack a which departs from such a notch with semi-axes b and c, with a and b in the same direction perpendicular to the (nominal) stress $\Delta\sigma$, is given by:

$$\Delta K_I = \eta\cdot F(a/b, c/b)\cdot\Delta\sigma\sqrt{\pi a} \qquad (22)$$
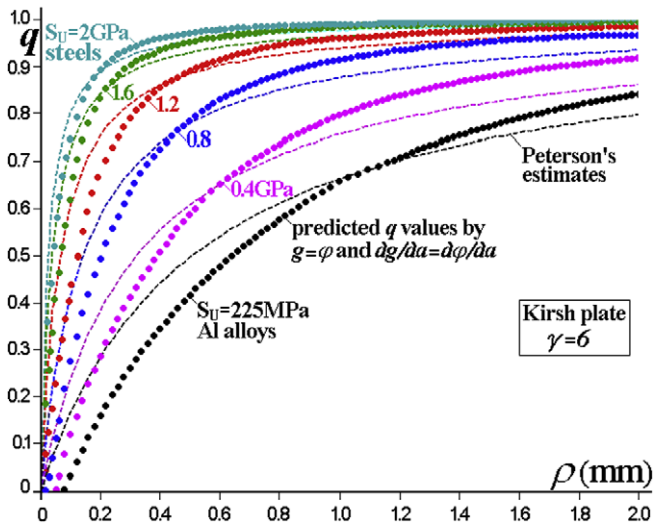
Fig. 6. Notch sensitivity q as a function of the Kirsh hole diameter ρ, estimated using mean ΔK_0, ΔS_0 and S_U from 450 steels and aluminium alloys and supposing $\gamma = 6$ [11].

where $\eta = 1.1215$ is the free surface correction factor and $F(a/b, c/b)$ is the geometric factor associated to the notch stress concentration effect, which can be calculated as a function of the non-dimensional parameter $s = a/(a + b)$ and of K_t, which is given by [21]:

$$K_t = \left(1 + 2\frac{b}{c}\right) \cdot \left[1 + \frac{0.1215}{(1 + c/b)^{2.5}}\right] \tag{23}$$

An analytical expression for the $F(a/b, c/b)$ of deep semi-elliptical notches with $c \leqslant b$ was fitted to a series of finite element numerical calculations as reported in [11], see Fig. 7:

$$F\left(\frac{a}{b}, \frac{c}{b}\right) \equiv f(K_t, s) = K_t \sqrt{\frac{1 - \exp(-K_t^2 \cdot s)}{K_t^2 \cdot s}}, \quad \text{for } c \leqslant b \tag{24}$$

A similar expression was also obtained for shallow semi-elliptical notches, with $c \geqslant b$:

$$F\left(\frac{a}{b}, \frac{c}{b}\right) \equiv f'(K_t, s) = K_t \sqrt{\frac{1 - \exp(-K_t^2 \cdot s)}{K_t^2 \cdot s}} \cdot [1 - \exp(-K_t^2)]^{-s/2},$$

$$\text{for } c \geqslant b \tag{25}$$

Making $g = \phi$ and $\partial g / \partial a = \partial \phi / \partial a$ in (21), it is possible to calculate the smallest stress range $\Delta\sigma$ (and the corresponding maximum non-

propagating crack size a associated with it) required to initiate and propagate a fatigue crack from the notch root for a given combination of γ and $\Delta K_0/\Delta S_0\sqrt{\rho}$, which can be used to calculate $K_f = \Delta S_0/\Delta\sigma$ and q. Indeed, in the lack of compressive residual stresses at the notch border, the mechanical reason for stopping a crack initiated at that border (when it reaches a size a_{st}) is the stress gradient near the notch root: to stop the crack it is necessary that the stress range decrease due to the gradient near the border overcomes the effect of increasing the crack size. In other words, under any stress range $\Delta\sigma < \Delta S_0/K_t$ a short crack $a < a_{st}$ departing from the notch boundary stops when it reaches
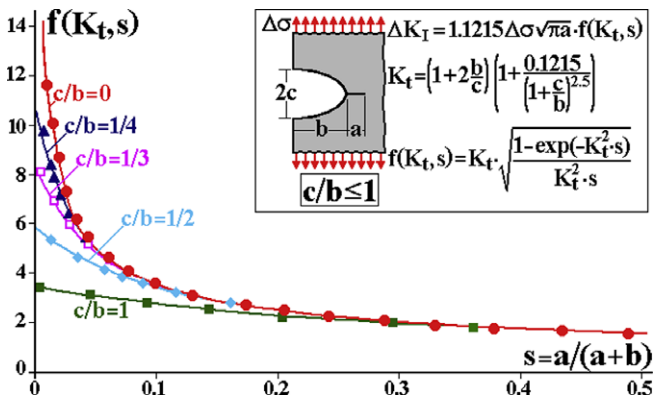
$$\Delta K_I = \eta \cdot \varphi(a_{st}) \cdot \Delta\sigma\sqrt{\pi a_{st}} = \Delta K_0 \cdot [1 + (a_0/a_{st})^{\gamma/2}]^{-1/\gamma} \tag{26}$$

It is important to emphasize that traditional notch sensitivity estimates, such as Peterson's $q = (1 + \alpha/\rho)^{-1}$, where α is a length obtained from the fitting of just seven experimental points, suppose that the sensitivity q depends only on the notch root ρ and the material ultimate strength S_U. However, as shown in Fig. 8, the sensitivity of semi-elliptical notches, besides depending on ρ, ΔS_0, ΔK_0 and γ, is also strongly dependent on the c/b ratio. Moreover, there are reasonable relationships between ΔS_0 and S_U, but not between ΔK_0 and S_U. This means that, e.g., two steels with same S_U but ΔK_0 widely different can behave in a way not predictable by the traditional estimates. The curves in Fig. 8 are calculated for typical Al alloys with mean ultimate strength $S_U = 225$ MPa, fatigue limit $S_L = 90$ MPa $\Rightarrow \Delta S_0 = 2S_L S_R/(S_L + S_R) = 129$ MPa, propagation threshold $\Delta K_0 = 2.9$ MPa $\sqrt{m}$, and $\gamma = 6$. Note that the corresponding Peterson's curve is well approximated by the semi-circular $c/b = 1$ notch.

5. The improved stop-hole model

An improved model for predicting the beneficial effect of the stop-holes on the crack re-initiation fatigue lives can be generated by using:

(i) a semi-elliptical notch with $b = 27.5$ mm and $\rho = c^2/b = 1, 2.5$ or 3 mm to simulate the stop-hole repaired specimens
(ii) the mechanical properties of the 6082 T6 Al alloy studied in this work
(iii) Eq. (21) to calculate the notch sensitivity and Eq. (14) for the stress intensity factor of the repaired specimens; and finally
(iv) K_f instead of K_t in the εN model expressed by Eqs. (7)–(11).

Fig. 7. Analytical expression for $f(K_t, s)$ fitted to finite elements numerical calculations of the stress intensity factors of cracks which depart from semi-elliptical notches with $b \geqslant c$ on the border of a semi-infinite plate loaded in mode I [11].
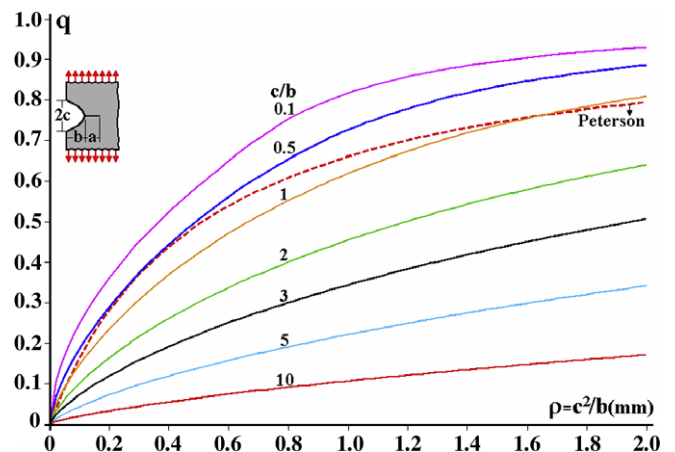
Fig. 8. Notch sensitivity q as a function of the semi-elliptical notch tip radius ρ for plates of typical Al alloys ($\Delta S_0 = 129$ MPa, $\Delta K_0 = 2.9$ MPa $\sqrt{m}$, $\gamma = 6$) loaded in mode I.

The predictions generated by such an improved model are presented in Figs. 9–11.
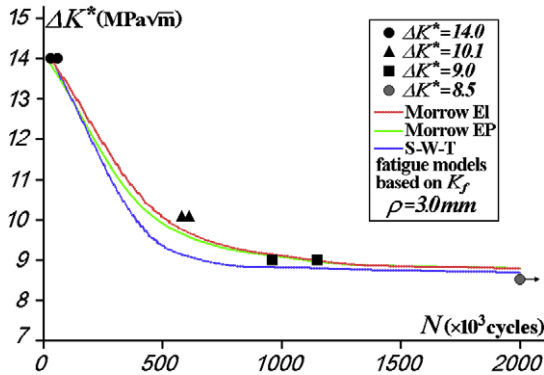
Fig. 9. Predicted and measured fatigue crack re-initiation lives at the roots of the stop-holes of radius $\rho = 3.0$ mm, using the fatigue stress concentration factor $K_f = 7.0$ of the repaired crack, taking in account the notch sensitivity of the involving semi-elliptical notch.
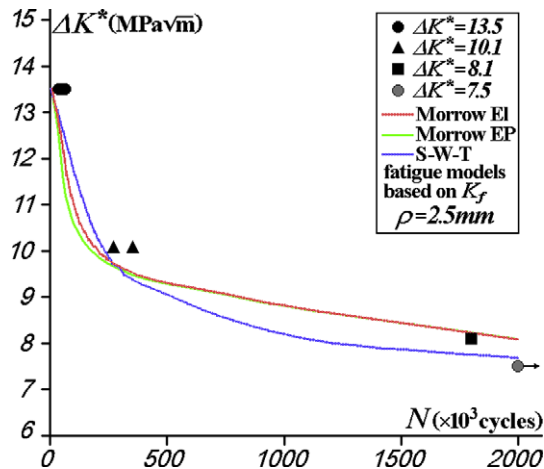
Fig. 10. Predicted and measured fatigue crack re-initiation lives for the repair stop-holes of radius $\rho = 2.5$ mm, using the fatigue stress concentration factor $K_f = 7.2$ calculated considering the notch sensitivity of the involving semi-elliptical notch.
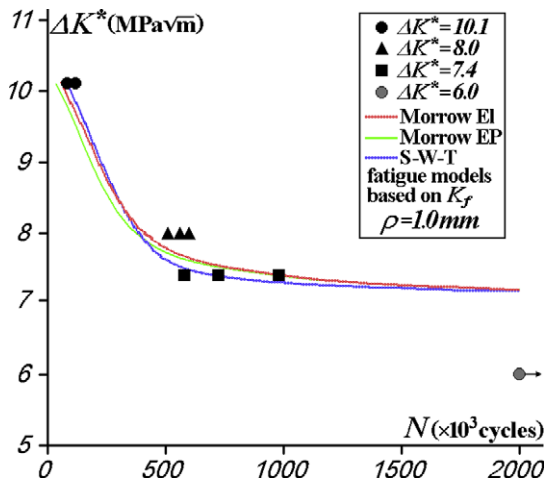
Fig. 11. Predicted and measured fatigue crack re-initiation lives at the roots of the stop-holes of radius $\rho = 1.0$ mm, using the fatigue stress concentration factor $K_f = 8.2$ of the repaired crack, taking in account the notch sensitivity of the involving semi-elliptical notch.

Since $q \cong 1$ for the $\rho = 3.0$ and $\rho = 2.5$ mm stop-holes, the predictions obtained using their calculated $K_f = 7.0$ and $K_f = 7.2$, respectively, are as good as those obtained using their estimated K_t, compare Fig. 9 with Figs. 3 and 10 with Fig. 4.

However, the overly conservative initial predictions for the smaller $\rho = 1$ mm stop-hole presented in Fig. 5, which were generated using its estimated $K_t \cong 11.5$, are much improved when the notch sensitivity effect quantified by its properly calculated $K_f = 8.3$ (considering the important influence of the elongated involving notch geometry) is used in the fatigue crack re-initiation calculations, as shown in Fig. 11.

The Al 6082 T6 fatigue limit and fatigue crack propagation threshold under pulsating loads required to calculate K_f are estimated as $\Delta K_0 = 4.8$ MPa $\sqrt{m}$ and $\Delta S_0 = 110$ MPa, following traditional structural design practices [7–10,22–25], and the Bazant's exponent was chosen, as recommended by [11], as $\gamma = 6$.

6. Conclusion

Classical εN techniques were used with properly estimated properties to reproduce the measured fatigue crack re-initiation lives after stop-hole repairing several modified SE(T) specimens. The predicted lives were not too dependent on the mean load εN model, and the larger stop-hole measured lives could be well reproduced using the stress concentration factor K_t in the Neuber/Ramberg–Osgood system. But such an approach yielded grossly conservative prediction for the smaller stop-hole life improvements. This problem was solved using the fatigue stress concentration factor K_f of the resulting notch instead of K_t in that system. However, the notch sensitivity q required to estimate K_f must be calculated in a proper way, considering the very important effect of the elongated notch geometry, since classical q estimates are only valid for approximately semi-circular notches.

References

[1] Ghfiri R, Amrouche A, Imad A, Mesmacque G. Fatigue life estimation after crack repair in 6005 AT-6 aluminium alloy using the cold expansion hole technique. Fatigue Fract Eng Mater Struct 2000;23:911.
[2] Song PS, Shieh YL. Stop drilling procedure for fatigue life improvement. Int J Fatigue 2004;26(12):1333–9.
[3] Domazet Z. Comparison of fatigue crack retardation methods. Eng Fail Anal 1996;3(2):137–47.
[4] Naned V, Stjepan J, Vatroslav G. Validation of crack arrest technique by numerical modeling. Int J Fatigue 1997;19(4):283–91.
[5] Murdani A, Makabe C, Saimot A, Kondou R. A crack-growth arresting technique in aluminum alloy. Eng Fail Anal 2008;15(4):302–10.
[6] Peterson RE. Stress concentration factors. Wiley; 1974.
[7] Shigley JE, Mischke CR, Budynas RG. Mechanical engineering design. 7th ed. McGraw-Hill; 2004.
[8] Juvinall RC, Marshek KM. Fundamentals of machine component design. 4th ed. Wiley; 2005.
[9] Norton RL. Machine design. An integrated approach. Prentice-Hall; 2005.
[10] Dowling NE. Mechanical behavior of materials. New Jersey: Prentice-Hall; 1999.
[11] Meggiolaro MA, Miranda ACO, Castro JTP. Short crack threshold estimates to predict notch sensitivity factors in fatigue. Int J Fatigue 2007;29(9-11):2022–31.
[12] E647 Standard test method for measurement of fatigue crack growth rates. ASTM Standards; 2006. [accessed 03.01.06].
[13] E399 Standard method of test for plain strain fracture toughness of metallic materials. ASTM Standards; 2006. [accessed 03.01.06].
[14] Borrego LP, Ferreira JM, Pinho da Cruz JM, Costa JM. Evaluation of overload effects on fatigue crack growth and closure. Eng Fract Mech 2003;70(11):1379–97.
[15] Meggiolaro MA, Castro JTP. Evaluation of the errors induced by high nominal stresses in the classical εN method. In: 8th International fatigue congress, Stockholm, Sweden, FATIGUE; 2002. pp. 2759–2766.
[16] Miranda ACO, Meggiolaro MA, Castro JTP, Martha LF, Bittencourt TN. Fatigue crack propagation under complex loading in arbitrary 2D geometries. ASTM STP 1411 2002;4:120–46.
[17] El Haddad MH, Topper TH, Smith KN. Prediction of non-propagating cracks. Eng Fract Mech 1979;11:573–84.

[18] Ciavarella M, Monno F. On the possible generalizations of the Kitagawa–Takahashi diagram and of the El Haddad equation to finite life. Int J Fatigue 2006;28(12):1826–37.

[19] Bažant ZP. Scaling of quasibrittle fracture: the fractal hypothesis, its critique and Weibull connection. Int J Fract 1996;83:41–65.

[20] Frost NE, Marsh KJ, Pook LP. Metal fatigue. Oxford: Clarendon Press; 1974 [Republished by Dover Pubblications, New York, 1999].

[21] Tada H, Paris PC, Irwin FR. The stress analysis of cracks handbook. Del Research; 1985.

[22] Juvinall RC. Engineering considerations of stress, strain, and strength. New York: McGraw-Hill; 1967.

[23] Stephens RI, Fatemi A, Stephens RR, Fuchs HO. Metal fatigue in engineering. 2nd ed. Interscience; 2000.

[24] Rice RC, editor. SAE fatigue design handbook. SAE; 1997.

[25] Park M. Fatigue failure of a hydraulic filter head. Eng Fail Anal 2002;9(4): 435–50.